frontiers in Immunology

ORIGINAL RESEARCH
published: 14 January 2021
doi: 10.3389/fimmu.2020.602284

Functional Characterization of Rare Genetic Variants in the N-Terminus of Complement Factor H in aHUS, C3G, and AMD

Edwin K. S. Wong[1,2†], *Thomas M. Hallam*[1,2†], *Vicky Brocklebank*[1,2], *Patrick R. Walsh*[1,2], *Kate Smith-Jackson*[1,2], *Victoria G. Shuttleworth*[1,2], *Thomas E. Cox*[1,2], *Holly E. Anderson*[1,2], *Paul Nigel Barlow*[3], *Kevin James Marchbank*[1,2], *Claire L. Harris*[1,2] *and David Kavanagh*[1,2,4*]

[1] Complement Therapeutics Research Group, Translational and Clinical Research Institute, Newcastle University, Newcastle upon Tyne, United Kingdom, [2] National Renal Complement Therapeutics Centre, Royal Victoria Infirmary, Newcastle upon Tyne, United Kingdom, [3] School of Chemistry, Joseph Black Building, University of Edinburgh, David Brewster Road, Edinburgh, United Kingdom, [4] NIHR Newcastle Biomedical Research Centre, Biomedical Research Building, Campus for Ageing and Vitality, Newcastle upon Tyne, United Kingdom

Membranoproliferative glomerulonephritis (MPGN), C3 glomerulopathy (C3G), atypical haemolytic uraemic syndrome (aHUS) and age-related macular degeneration (AMD) have all been strongly linked with dysfunction of the alternative pathway (AP) of complement. A significant proportion of individuals with MPGN, C3G, aHUS and AMD carry rare genetic variants in the *CFH* gene that cause functional or quantitative deficiencies in the factor H (FH) protein, an important regulator of the AP. *In silico* analysis of the deleteriousness of rare genetic variants in *CFH* is not reliable and careful biochemical assessment remains the gold standard. Six N-terminal variants of uncertain significance in *CFH* were identified in patients with these diseases of the AP and selected for analysis. The variants were produced in *Pichia Pastoris* in the setting of FH CCPs 1–4, purified by nickel affinity chromatography and size exclusion and characterized by surface plasmon resonance and haemolytic assays as well as by cofactor assays in the fluid phase. A single variant, Q81P demonstrated a profound loss of binding to C3b with consequent loss of cofactor and decay accelerating activity. A further 2 variants, G69E and D130N, demonstrated only subtle defects which could conceivably over time lead to disease progression of more chronic AP diseases such as C3G and AMD. In the variants S159N, A161S, and M162V any functional defect was below the capacity of the experimental assays to reliably detect. This study further underlines the importance of careful biochemical assessment when assigning functional consequences to rare genetic variants that may alter clinical decisions for patients.

Keywords: complement factor H, age-related macular degeneration, aHUS, C3G, MPGN

OPEN ACCESS

Edited by:
Nicole Thielens, UMR5075 Institut de Biologie Structurale (IBS), France

Reviewed by:
Margarita López-Trascasa, Autonomous University of Madrid, Spain
Christine Skerka, Leibniz Institute for Natural Product Research and Infection Biology, Germany

***Correspondence:**
David Kavanagh
david.kavanagh@ncl.ac.uk

†These authors have contributed equally to this work

Specialty section:
This article was submitted to Molecular Innate Immunity, a section of the journal Frontiers in Immunology

Received: *02 September 2020*
Accepted: *25 November 2020*
Published: *14 January 2021*

Citation:
Wong EKS, Hallam TM, Brocklebank V, Walsh PR, Smith-Jackson K, Shuttleworth VG, Cox TE, Anderson HE, Barlow PN, Marchbank KJ, Harris CL and Kavanagh D (2021) Functional Characterization of Rare Genetic Variants in the N-Terminus of Complement Factor H in aHUS, C3G, and AMD. Front. Immunol. 11:602284. doi: 10.3389/fimmu.2020.602284

INTRODUCTION

Atypical haemolytic uraemic syndrome (aHUS) (1), membranoproliferative glomerulonephritis (MPGN), C3 glomerulopathy (C3G) (2) and age-related macular degeneration (AMD) (3) are all diseases that have been associated with dysregulation of the alternative pathway (AP) of complement.

The hallmark pathological lesion in aHUS is thrombotic microangiopathy within the kidney, characterized by the clinical features of microangiopathic haemolytic anaemia, thrombocytopenia and acute kidney failure (1). Conversely, MPGN and C3G are a group of conditions in which deposition of complement activation products within the glomerulus occurs, resulting in nephrotic/nephritic syndrome and chronic progressive renal failure (2). Specifically, MPGN is a pattern of glomerular injury, involving thickening of the glomerular capillary wall and an increase in mesangial components. C3G is the current preferred term when the glomerular staining is predominantly C3 positive by immunofluorescence. Dense deposit disease is a special sub-type of C3G, characterized by prominent intramembranous laminar deposits that are visible on electron microscopy, associated historically with MPGN (2).

AMD is the leading cause of irreversible vision loss in elderly Caucasian populations. It is characterized by lipoprotein-rich drusen deposits that form in the subretinal space and the recruitment of immune cells, such as microglia and macrophages (4, 5). Degeneration and geographic atrophy of the retinal pigment epithelium and photoreceptors occur in the macula of the retina in advanced dry AMD, while advanced wet AMD involves angiogenesis in the choroid and subsequent choroidal neovascularization (6).

Genetic studies have linked common (7–11) and rare genetic variants (12–17) in the complement factor H gene (*CFH*) to all of these conditions. Complement factor H (FH) is an abundant fluid phase regulator of the AP, and functions as a cofactor for factor I (FI) in the cleavage of the activated central molecule of the pathway, C3b (18, 19). Screening for rare genetic variants in *CFH* has been established in clinical practice to determine a possible genetic cause of disease. Knowledge of *CFH* variants and their functional significance plays an important role in understanding prognosis (20) and determining the risk of disease recurrence after renal transplantation (21) in aHUS. Similar genotype-phenotype correlations have not yet been established in MPGN/C3G. In all of these diseases, common risk haplotypes also associate with pathology and play a role in genetic susceptibility (7–11).

The functional consequences of genetic variants identified in individual patients needs to be carefully considered as they could influence the approach to clinical management of the condition. Because each genetic variant is rare, there may not be any literature reports on its functional impact. There is thus a good case for a robust and consistent procedure to be established for assessing the likelihood that a rare variant in *CFH* is functionally detrimental and hence could be contributing to disease. Functional testing although time-consuming remains the gold standard for attributing significance to a rare genetic variant and has been shown to be contradictory to *in silico* analysis of variants in *CFH* (22).Most rare *CFH* genetic variants in aHUS reported to date have been found to code for amino acids in the C-terminal recognition domain, comprising complement control proteins (CCPs) 19–20 (23). Many variants have been extensively studied in the laboratory and most demonstrate functional significance (14, 24). Variants have also been reported in the N-terminal regulatory domain, comprising CCPs 1–4 and there is significant enrichment of N - terminal variants in AMD (25). To date, there have been functional studies of 10 variants in CFH CCPs 1-4, namely; R53C (16, 22), R53H (15, 26, 27), R53P (22), R53S (22), S58A (22), I62V (15, 27, 28), R78G (15), R83S (13), D90G (16) and Del K224 (29), and in many cases there was a severe loss of function.

The objective of this study was to expand this knowledge pool by testing the functional significance of other variants of uncertain significance identified in the N-terminal region of FH in patients with aHUS, MPGN, C3G, and AMD.

MATERIALS AND METHODS

Selection of N-Terminal *CFH* Variants for Functional Study

At the time of study inception, the literature was reviewed for N-terminal rare genetic variants described in the complement mediated diseases: MPGN/C3G; aHUS, and AMD. Six N-terminal heterozygous variants known to result in normal serum FH levels and for which no prior functional data were available were selected as follows: G69E (17, 25), Q81P (30), D130N (25, 31), S159N (25, 32, 33), A161S (25, 30, 31, 33, 34) and M162V (35).

Production and Purification of Proteins

Clones of *Pichia pastoris* strain KM71H producing wild-type (WT) and mutant (G69E, Q81P, D130N, S159N, A161S, and M162V) protein in the setting of CCPs1–4 were generated as described previously (15). In brief, each point mutation was generated in a pPICZαB (Invitrogen) vector containing residues 19–263 of FH (which encodes CCPs 1–4 of mature FH; residues 1–18 are the mammalian signal peptide), with a C-terminal 6x His tag and an N-terminal myc tag (EQKLISEEDL) using QuikChange site-directed mutagenesis kit (Stratagene). Fidelity was confirmed by bi-directional Sanger sequencing. KM71H cells were transformed using electroporation, selected for by zeocin, and screened for protein expression.

Protein expression was carried out in a 3L BioFlo 115 Biofermenter (New Brunswick). A starter culture was transferred into 1L of basal fermentor salts (0.095%) (w/v) calcium sulphate, 1.82% (w/v) potassium sulphate, 1.5% (w/v) magnesium sulphate heptahydrate, 0.42% (w/v) potassium hydroxide, 2.7% (v/v) phosphoric acid and 2.5% (v/v) glycerol) enriched with 1% (w/v) casein amino acids, 0.5% (w/v) PTM1 salts and 0.5% (v/v) antifoam A (Sigma). After the initial batch fed glycerol was exhausted, software-controlled glycerol feeds were maintained for 24 h at 30°C. The cells were allowed to

starve for 4 h before recombinant expression was induced with 0.75% methanol containing 0.5% (w/v) PTM1 salts. After three days at 15°C with software-controlled methanol feeds, cells were spun out and the supernatant was removed, filtered and its pH adjusted to 7.4.

The supernatant was then applied to a 5ml His-Trap FF column (GE-healthcare) at 4°C and the protein eluted with 500 mM imidazole followed by size exclusion chromatography using a HiLoad® 16/600 Superdex® 200 pg column (GE Healthcare) (**Supplementary Figure 1**). Protein concentrations were calculated using absorbance at 280 nm and a calculated extinction coefficient (478,70M cm^{-1}).

Binding Affinity for C3b by Surface Plasmon Resonance

The binding affinities of the WT and mutant FH1-4 proteins to C3b were monitored by SPR using a Biacore X100 instrument (GE Healthcare) (14). A total of 300 resonance units of human C3b (CompTech) were immobilized on a Biacore series S-CM5 sensor chip (GE Healthcare) using standard amine coupling. The reference surface of the chip was prepared by performing a mock coupling in the absence of any protein. Experiments were performed at 25°C and 30 µl/min flow rate. Duplicate injections (concentrations up to 40 µM) were performed in 10 mM HEPES-buffered saline, 3 mM EDTA, 0.05% (v/v) surfactant p20 (GE Healthcare). A contact time of 45s was used (sufficient for achieving steady state conditions for most samples) followed by a dissociation period of 90 s. Chips were regenerated between sample injections, with one 45 s injections of 1 M NaCl, pH 7.0. Data were processed using the BIAevaluation 4.1 software (GE Healthcare). Data from the reference cell and a blank (buffer) injection were subtracted and dissociation constants calculated using a steady-state affinity model from the background-subtracted traces.

Measurement of Decay Acceleration Activity by Surface Plasmon Resonance

Decay accelerating activity (DAA) was measured in real-time using a Biacore X100 instrument as described previously (15). Briefly, 300 resonance units of C3b were immobilized using standard amine coupling to the CM5 sensor chip. Subsequently, a mixture of FB (250 nM) and FD (30 nM) was flowed (10 µl/min) over the surface for 120s to form the AP convertase.

The convertase was allowed to decay naturally for 210s and then FH1-4 (WT or variants at 166nM) [in running buffer, HEPES-buffered saline containing 0.5% (v/v) surfactant P20 and 1 mM $MgCl_2$, Temp 25°C] was flowed across the surface for 60s, and convertase decay was visualized in real time. Between injections, surfaces were regenerated using a 45s injection of 1µM purified FH (CompTech) followed by a 45s injection of 1M NaCl, pH7.0. Data were evaluated using BIAevaluation 4.1 (GE Healthcare).

Cofactor Assay in the Fluid Phase

In vitro fluid phase assays were used to measure cofactor activity (CA) for FI-mediated proteolytic cleavage of C3b (14). FI and C3b were purchased from CompTech. An aliquot of 3µL of C3b (5.68 µM), 4.5 µL of FI (0.114 µM) and 5 µL of FH1-4 (0.75 µM) were made up to a final volume of 15µL in phosphate buffered saline (PBS). For the negative control 5 µL of PBS was used. The mixture was incubated at 37°C for 15 min, and the reaction stopped by the addition of 2x Laemmli reducing buffer to a final volume of 30 µL and heated to 95°C for 5 min. The products of the reaction were then separated by SDS-PAGE and revealed using Coomassie Blue staining.

Measuring Decay Acceleration on Sheep Erythrocytes

C3b-coated sheep erythrocytes (EA-C3b) were prepared as described previously (13). Cells were resuspended to 2% (v/v) in AP buffer (5 mM sodium barbitone, pH 7.4, 150 mM NaCl, 7 mM $MgCl_2$, 10 mM EGTA). The AP convertase was formed on the cell surface by incubating 50µL of cells with an equal volume of AP buffer containing FB (40µg/ml) and FD (0.4 µg/ml; CompTech) at 37°C for 15 min. Cells (100 µl) were incubated with 50 µl of a concentration range of FH1–4 (WT or variants) in PBS/20 mM EDTA for 15 min. Lysis was developed by adding 50 µl of 4% (v/v) normal human serum depleted of FB and FH (NHSΔBΔH) (13) in PBS/20 mM EDTA and incubating at 37°C for 60 min. To determine the amount of lysis, cells were pelleted by centrifugation, and hemoglobin release was measured at 410 nm (A410). Controls included 0% lysis (buffer only) and 100% lysis (0.1% (v/v) Nonidet P-40), Percentage of inhibition from lysis was calculated by the formula (A_{410}[buffer only]-A_{410}[FH])/A_{410}[buffer only]*100%.

Measuring Cofactor Activity on Sheep Erythrocytes

To test CA (13), washed EA-C3b cells were resuspended to 2% (v/v) in AP buffer and incubated with an equal volume of a range of concentrations of FH1–4 (WT and variants) and 2.5 µg/ml FI (CompTech) for 15 min at 25°C. After three washes in AP buffer, a 50 µl aliquot of cells (2%) was mixed with 50 µl AP buffer containing FB (40 µg/ml) and FD (0.4 µg/ml) and then incubated for 15 min at 25°C to form AP convertase on the remaining C3b. Lysis was developed by adding 50 µl of 4% (v/v) NHSΔBΔH in PBS/20 mM EDTA and incubating at 37°C for 10 min. Percentage of inhibition from lysis was calculated by the formula (A_{410}[buffer only]-A_{410}[FH])/A_{410}[buffer only]*100%.

RESULTS

Expression of Recombinant FH1-4 Variants

The rare genetic variants, G69E, Q81P, D130N, S159N, A161S, and M162V were analyzed in the setting of a construct containing the first four CCP domains of FH responsible for C3b binding, DAA, and CA (**Figure 1**). This allowed interrogation of the functional consequences of variants in the N-terminal region of FH without the confounding presence of the C-terminal region, CCP19-20, which contains a second,

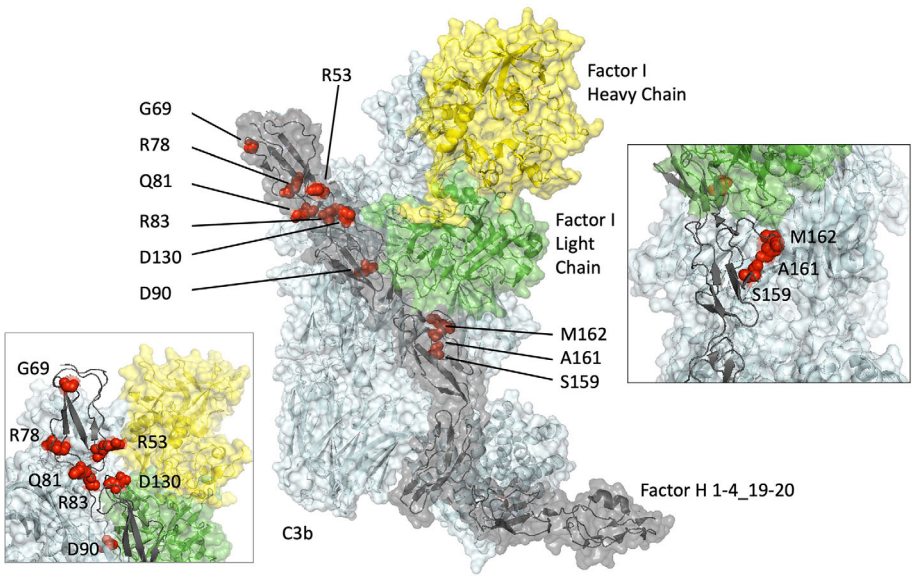

FIGURE 1 | Structural modelling of rare genetic variants in an x-ray–derived co-crystal structure of Factor H CCP1-4_19-20/C3b/Factor I displayed using PyMOL (V2.0.6, Schrödinger, LLC). The amino acids altered by the rare genetic variations analyzed in this study (G69, Q81, D130, S159, A161, M162) and previously (R53 (15, 16, 22), R78 (15), R83 (13), D90 (16)) (red spheres) are shown within a co-crystal structure of Factor I (heavy chain: yellow, light chain: green), Factor H (grey) and C3b (cyan). (Protein Database ID code 5O32) (36).

stronger, C3b binding site. We have previously validated this strategy in N terminal *CFH* variants by demonstrating equivalent results in the setting of both full-length recombinant FH and the CCP1-4 recombinant FH construct used in this study (15, 27).

In keeping with the normal FH serum levels reported for these variants, all six of them were produced as folded, soluble proteins by genetically modified *Pichia pastoris*. Following purification, all FH1-4 samples were free of aggregates and degradation (**Supplementary Figure 1**).

Effect of Variants on C3b Binding

Surface plasmon resonance (SPR) was used to measure the binding interaction between FH1-4 and immobilized C3b. The plots of maximum binding response (RUs) versus concentration, used to estimate K_D values, are shown for FH1–4 WT (**Figures 2A, B**); FH1–4 G69E (**Figure 2C**); FH1–4 Q81P (**Figure 2D**); FH1–4 D130N (**Figure 2E**); FH1–4 S159N (**Figure 2F**); FH1–4 A161S (**Figure 2G**); FH1–4 M162V (**Figure 2H**).

The variant FH1-4 Q81P showed no detectable binding to C3b at the highest concentration available (40 μM Q81P in the solution flowed over the chip). All the other variants bound to C3b with a strength comparable to that of WT FH1-4. As a ratio of the K_D for C3b of WT FH1-4, K_D values were 1.2-fold for G69E, 1.4-fold for D130N, 1.2-fold for S159N, 0.97-fold for A161S and 1.2-fold for M162V (**Table 1**).

Co-Factor Activity of FH1-4 to C3b

To assess the effect of these sequence variations on co-factor activity, fluid-phase CA assays were initially undertaken. These demonstrated that FH1–4 Q81P has minimal CA, judging by the relative strength of the intact α' substrate band of C3b on an SDS-polyacrylamide gel, and minimal formation of the α1 cleavage products (**Figure 3**). In these semi quantitative assays, the remaining variants demonstrated co-factor activity similar to that of WT FH1-4.

The activity of each rare variant as a co-factor in the FI-mediated proteolytic cleavage of surface-bound C3b was then assessed on sheep erythrocytes. Again, Q81P FH1-4 exhibited the poorest co-factor activity (IC_{50} 11x > that of WT, **Figure 4B**). The other variants tested had surface CAs comparable to WT CA (**Figures 4A, E, F**), although D130N (IC_{50} 1.66x greater than WT) (**Figure 4C**) and S159N (IC_{50} 1.54x greater than WT) (**Figure 4D**), showed small reductions in function.

Decay Acceleration Activity of FH1-4 to C3b

The effect of sequence variants on the ability of FH1-4 to accelerate decay of the C3 convertase (C3bBb) assembled on the surface of sheep erythrocytes was also analyzed. These assays revealed an approximately 25-fold reduction in activity of the FH1–4 Q81P compared with FH1–4 WT (**Figure 5B**). FH-D130N displayed a small decrease in surface DAA activity (IC_{50} 2x WT) (**Figure 5C**). The remaining variants displayed still smaller differences (IC_{50}: G69E 1.3x WT; S159N 0.9X WT; A161S 1.3X WT; M162V, 1.02X WT) (**Figure 5**).

The effect of the six sequence variations in FH 1-4 on DAA was also analyzed in real time on an SPR chip surface (**Figures 6A–F**). In this assay the FH1–4 Q81P variant demonstrated only minimal if any effect on the rate of C3bBb decay (**Figure 6B**). Consistent with DAA measurements on erythrocytes, D130N

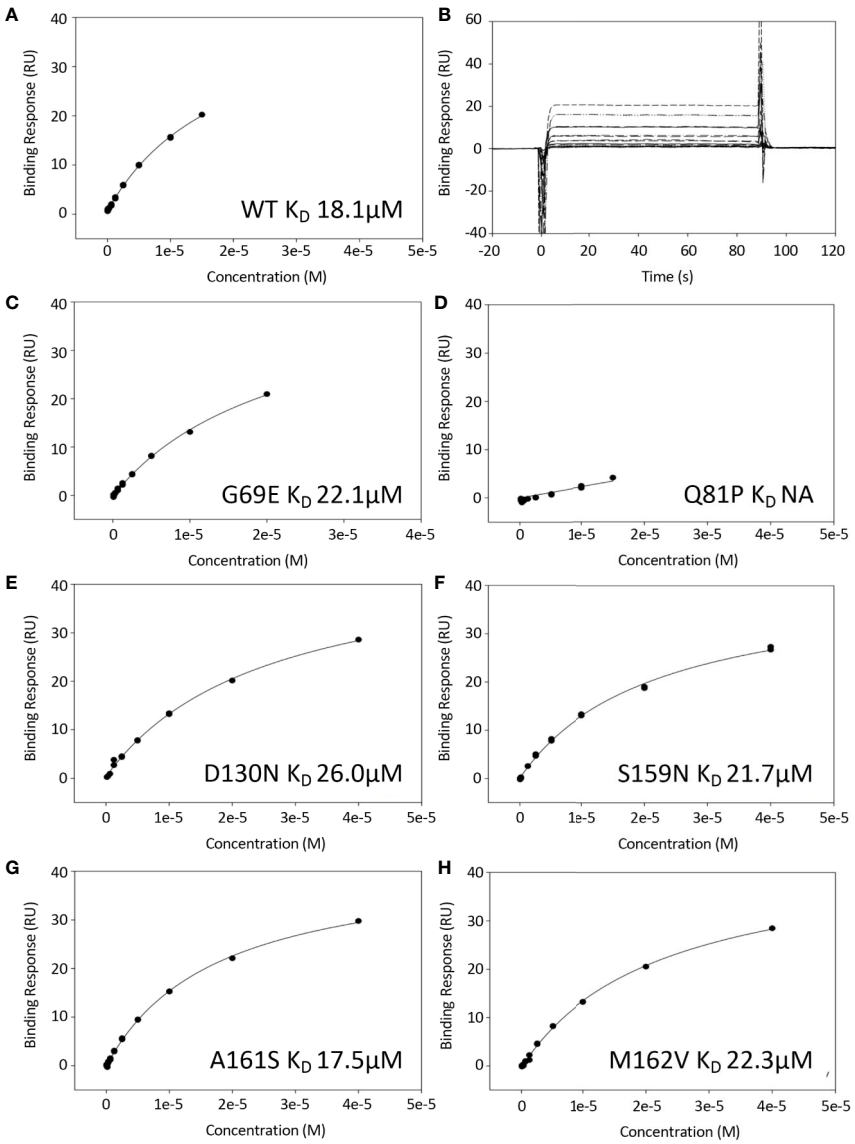

FIGURE 2 | Binding of FH1-4 to C3b using surface plasmon resonance. C3b was immobilized to a CM5 sensor chip (300RU) and FH1-4 (WT and variants) were injected across (concentrations up to and including 40uM). **(B)** Sensorgrams from WT experiment demonstrating rapid association/disassociation of FH1-4 to with/from C3b. This is representative of interactions from all variants. The steady state response was plotted against concentration for all variants and shown in **(A, C–H)**. All have similar K_D except for Q81P where there was minimal binding at the concentrations used.

TABLE 1 | Summary of the functional effects of each N-terminal *CFH* variant.

Variant	Disease	Effect of variant on				
		Affinity to C3b (Kd xWT)	Decay on SPR Assay	Decay on Sheep E (IC_{50} xWT)	Co-factor Fluid Phase	Co-factor on Sheep E (IC_{50} xWT)
G69E	AMD	1.2	↓	1.3	↔	1.1
Q81P	aHUS	↓	↓	25.1	↓	11.0
D130N	C3G, AMD	1.44	↓	2.0	↔	1.66
S159N	aHUS, AMD	1.20	↔	0.9	↔	1.54
A161S	aHUS, C3G, AMD	0.97	↔	1.3	↔	1.26
M162V	aHUS	1.23	↔	1.02	↔	1.48

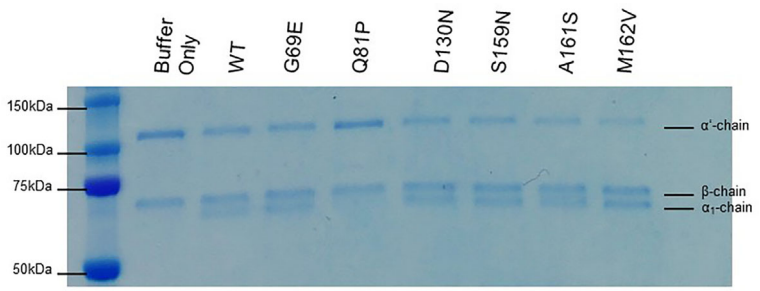

FIGURE 3 | Fluid phase co-factor activity. C3b, FI, and FH1-4 were incubated for 30 min at 37°C before the addition of 2x Laemmli to stop the co-factor reaction. The products of the reaction are visualized following separation by SDS-PAGE and staining with Coomassie blue. Q81P clearly has minimal co-factor activity in the fluid phase. All other variants have detectable co-factor activity by the loss of the α' band and the appearance of the α1 band. The β chain is the internal control. Data representative of at least 3 repeats.

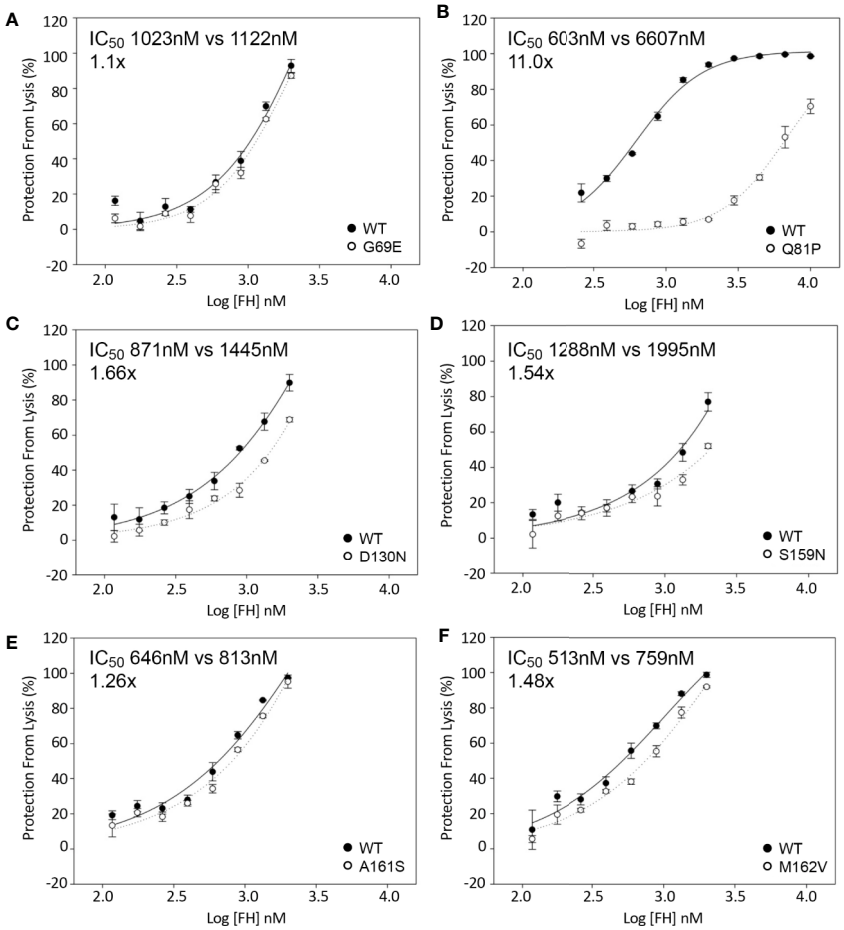

FIGURE 4 | Inactivation of C3b on the surface of sheep erythrocytes. FH1-4 and FI was incubated with sheep erythrocytes with preformed surface C3b for 15 min at 25°C. Following wash steps, C3 convertase was formed on the remaining intact C3b before the instigation of lysis by the addition of ΔBHNHS. Protection from lysis was calculated as [A_{410}(buffer only)–A_{410}(FH)/A_{410}(buffer only)*100]. **(B)** Q81P has large effect on co-factor activity compared to WT (IC_{50} 11x). **(C)** D130N demonstrated a slight loss of activity (IC_{50} 1.66x). The remaining variants demonstrated similar activity **(A, D–F)**.

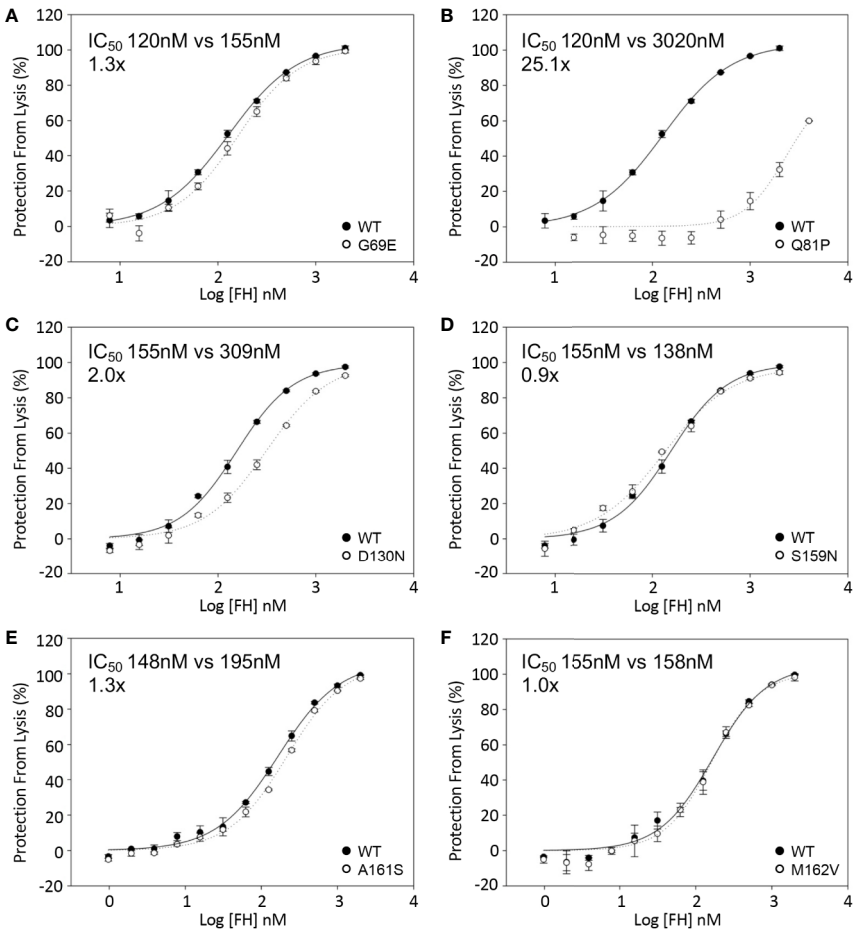

FIGURE 5 | Decay acceleration of C3 convertase formed on surface of sheep erythrocytes. FB and FD were incubated with sheep erythrocytes with preformed surface C3b. The cells were then incubated with FH1-4 for 15 min at 25°C before the addition of ΔBHNHS to instigate lysis. Protection from lysis was calculated as [A_{410}(buffer only)–A_{410}(FH)/A_{410}(buffer only)*100]. **(B)** Q81P has a profound effect of DAA with an IC_{50} 25-fold greater than wild type. The IC_{50}' s relative to WT were **(A)** 1.3x, G69E **(C)** 2x, D130N **(D)** 0.9x, S159N **(E)** 1.3, A161S **(F)** 1x, M162V.

FH1-4 had slightly less activity than WT (**Figure 6C**), as does G69E FH1-4 has less DAA than WT (**Figure 6A**).

DISCUSSION

The cost and speed of next-generation sequencing has now reached the point where this evolving technology can be used to alter clinical management in real time. While the results of sequencing results may be available rapidly, their interpretation can be difficult.

While the functional significance of large gene rearrangements, or frameshift mutations is clear-cut and the use of curated locus specific databases (e.g. https://www.complement-db.org/home.php) may provide data on previously described genetic variants (37), many variations in *CFH* consist of missense mutations or potential splice site changes not seen before. Interpreting these variants of unknown significance (VUSs) is particularly challenging (37).

In silico prediction of the consequences of amino acid changes may be attempted but in at least one *CFH* (22) case, these have proved unreliable. In the current study we provide detailed functional analysis of six rare genetic variants in the N-terminus of *CFH* that have been described in aHUS, C3G/MPGN and AMD.

The only one of these variants that had a profound effect on the complement regulatory functions of FH1-4 was Q81P, described in aHUS. It is apparent from the SPR results that its affinity for C3b is very weak compared to that of WT FH. The low affinity observed between Q81P and C3b agrees with inferences based on a co-crystal structure of C3b and CFH1–4 (36, 38) (**Figure 1**), which displays that Q81 is at the surface of the FH1-4 molecule, and is close to putative binding sites on C3b, similar to R83, a change to which (R83S) we have shown to be highly deleterious (13). In keeping with its inability to bind well to C3b, Q81P had a profound negative (25.1-fold and 11.0-fold) effect on DAA and CA, respectively. The proximal section of CCP2 and the CCP1-CCP2 linker region within FH interact through hydrophobic

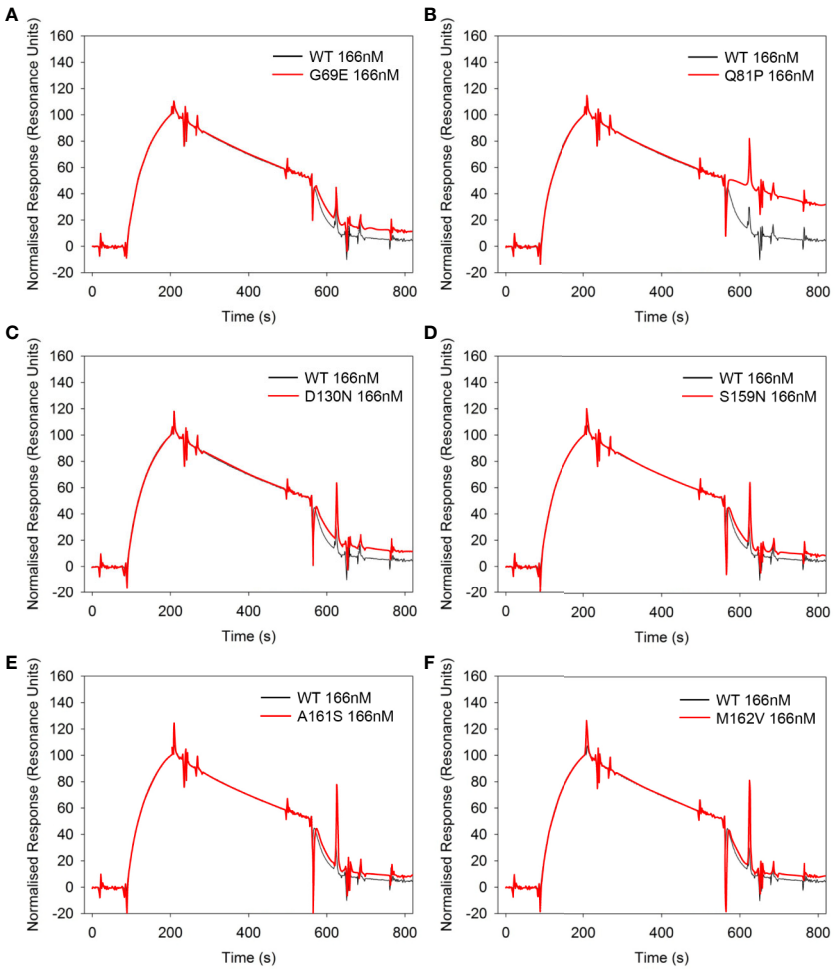

FIGURE 6 | Decay acceleration of C3 convertase in real time using surface plasmon resonance. FB and FD were injected over the surface of immobilized C3b (300RU) to form a convertase as shown by an initial increase in resonance units. The convertase was allowed to decay naturally for 120s before an injection of 166nM of each FH1-4 variant **(A–F)**. All variants show the ability to accelerate decay of the AP C3 convertase apart from Q81P **(B)**. Compared to WT, G69E **(A)** and D130N **(C)** appear to be slightly less effective. Data representative of at least 2 repeats. Variant curves highlighted in red.

interactions and salt bridges to the α' NT and MG7 domain of C3b. Q81 occupies this interface along with R78 and R83 that (when substituted by G and S respectively) also display markedly reduced affinity for C3b with consequent loss of DAA and CA (**Figure 1**).

This analysis is particularly interesting as it demonstrates that 3 variants in the same region of FH all lead to a profound defect in C3b binding with consequent abrogation of complement regulation yet cause different diseases: aHUS (R78G (15); Q81P) and C3G (R83S (13)). This suggests that the phenotype associated with these regulatory defects can be modified by genetic and environmental factors as demonstrated by Recalde et al. (39).

The G69E variation, also in CCP 1, was described in AMD. Unsurprisingly, given its location on the opposite face from the FH/C3b interface (**Figure 1**), the affinity for C3b was unaltered and there was no or only a very minor defect in CA (in the fluid phase and on cell surfaces) and there was only a subtle defect in DAA. In CCP2, D130N is predicted to be in a FH/C3b groove that allows binding of FI and subsequent cleavage of C3b, but only a small effect on co-factor activity (IC_{50} 1.66x) was observed for this variant in the sheep erythrocyte assay. Furthermore, the D130N variant produced a small but consistent effect on decay acceleration as observed on the SPR-based and cell lysis assay: such an effect on decay without loss of C3b binding has been reliably demonstrated in studies of R53H in aHUS and R53C, a variant that has been reported in association with aHUS, MPGN, C3G and AMD (16, 22, 25, 31, 32, 40) In these studies, however, there was a profound loss of DAA, suggesting the critical role of R53 in DAA. Whilst we have shown that there is an effect due to the D130N and G69E variants, the magnitude of the effect is much smaller than in causative N-terminal variants described in aHUS. This would be consistent with a minor overactivation of the AP of complement in a process that is thought to occur in

more chronic disease, as observed in both of these rare variants (G69E, AMD and D130N, C3G).

Of the other variants, none displayed a detectable loss of function. Within CCP3; S159N; A161S; and M162V do sit at the interface with C3b but they displayed similar affinities for C3b as WT FH1-4 (**Figure 1**). They also displayed DAA and CA of a similar order of magnitude to WT FH1-4. The S159N and A161S variants have been demonstrated to occur in excess in AMD-case cohorts (versus control) (25) and it is possible that even the very small variations versus WT contribute to a chronic low-level complement overactivity leading to slow accumulations of complement-mediated damage over a long period of time. The minor differences that were observed were not reproducible across different assays for CA or DAA and therefore we conclude that any difference is below the detection capability of our assays.

As with previous studies *in silico* analysis here proved unreliable (22) with the profoundly perturbed Q81P variant classified as "tolerated" or a "polymorphism" in some analyses while the S159N variant (with normal function) was classified as "possibly damaging" in other analysis (**Supplementary Table 1**). As such *in silico* analysis may still be applied but should be interpreted with great caution especially when used in clinical management of disease.

In summary, we identify significant abrogation of function in an N-terminal variant of FH, Q81P, which is likely to be causative of aHUS. Two variants, G69E and D130N, demonstrated minor defects in complement regulation, which could conceivably over time lead to disease progression of more chronic diseases i.e. in C3G and AMD. Conversely, in the S159N, A161S, and M162V any functional defect was below the capacity of the experimental assays to reliably detect. This study further underlines the importance of careful biochemical assessment of disease-associated variants in complement proteins through a battery of functional assays.

DATA AVAILABILITY STATMENT

The raw data supporting the conclusions of this article will be made available by the authors, without undue reservation.

AUTHOR CONTRIBUTIONS

All authors listed have made a substantial, direct, and intellectual contribution to the work and approved it for publication.

FUNDING

The research was supported/funded by NIHR Newcastle Biomedical Research Centre at Newcastle upon Tyne Hospitals NHS Foundation Trust. DK was funded by Fight for Sight, the Wellcome Trust, the Medical Research Council, Kidney Research UK and Complement UK. CLH was funded by the Medical Research Council. EKSW was funded by Northern Counties Kidney Research Fund and was an MRC clinical research fellow and an NIHR Academic Clinical Lecturer. TMH is funded by Complement UK. VB is a Medical Research Council/Kidney Research UK Clinical Research Training Fellow (MR/R000913/1. PW is funded by the Wellcome trust. KSJ is a Medical Research Council (MRC) clinical research fellow (MR/R001359/1). TEC is funded by MRC Discovery Medicine North. KJM was funded by the Northern Counties Kidney Research Fund, the Newcastle Healthcare Charites and a Kidney Research UK project grant (RP7/2015).

ACKNOWLEDGMENTS

We thank Jennifer A. Hart for her technical assistance with figure generation. We would are also grateful to Helen Waller for her help with the BIAcore work presented in this study.

SUPPLEMENTARY MATERIAL

The Supplementary Material for this article can be found online at: https://www.frontiersin.org/articles/10.3389/fimmu.2020.602284/full#supplementary-material

REFERENCES

1. Brocklebank V, Wood KM, Kavanagh D. Thrombotic Microangiopathy and the Kidney. *Clin J Am Soc Nephrol* (2018) 13(2):300–17. doi: 10.2215/CJN.00620117
2. Wong EKS, Kavanagh D. Diseases of complement dysregulation-an overview. *Semin Immunopathol* (2018) 40(1):49–64. doi: 10.1007/s00281-017-0663-8
3. Tzoumas N, Hallam D, Harris CL, Lako M, Kavanagh D, Steel DHW. Revisiting the role of factor H in age-related macular degeneration: insights from complement-mediated renal disease and rare genetic variants. *Surv Ophthalmol* (2020) S0039-6257(20)30146-6. doi: 10.1016/j.survophthal.2020.10.008
4. Combadiere C, Feumi C, Raoul W, Keller N, Rodero M, Pezard A, et al. CX3CR1-dependent subretinal microglia cell accumulation is associated with cardinal features of age-related macular degeneration. *J Clin Invest* (2007) 117 (10):2920–8. doi: 10.1172/JCI31692
5. Cursiefen C, Chen L, Borges LP, Jackson D, Cao J, Radziejewski C, et al. VEGF-A stimulates lymphangiogenesis and hemangiogenesis in inflammatory neovascularization via macrophage recruitment. *J Clin Invest* (2004) 113(7):1040–50. doi: 10.1172/JCI20465
6. Ambati J, Fowler BJ. Mechanisms of age-related macular degeneration. *Neuron* (2012) 75(1):26–39. doi: 10.1016/j.neuron.2012.06.018
7. Hageman GS, Anderson DH, Johnson LV, Hancox LS, Taiber AJ, Hardisty LI, et al. A common haplotype in the complement regulatory gene factor H (HF1/CFH) predisposes individuals to age-related macular degeneration. *Proc Natl Acad Sci USA* (2005) 102(20):7227–32. doi: 10.1073/pnas.0501536102
8. Edwards AO, Ritter R,3, Abel KJ, et al. Complement factor H polymorphism and age-related macular degeneration. *Science* (2005) 308(5720):421–4. doi: 10.1126/science.1110189
9. Haines JL, Hauser MA, Schmidt S, et al. Complement factor H variant increases the risk of age-related macular degeneration. *Science* (2005) 308 (5720):419–21. doi: 10.1126/science.1110359

10. Klein RJ, Zeiss C, Chew EY, et al. Complement factor H polymorphism in age-related macular degeneration. *Science* (2005) 308(5720):385–9. doi: 10.1126/science.1109557
11. Pickering MC, de Jorge EG, Martinez-Barricarte R, et al. Spontaneous hemolytic uremic syndrome triggered by complement factor H lacking surface recognition domains. *J Exp Med* (2007) 204(6):1249–56. doi: 10.1084/jem.20070301
12. Warwicker P, Goodship TH, Donne RL, et al. Genetic studies into inherited and sporadic hemolytic uremic syndrome. *Kidney Int* (1998) 53(4):836–44. doi: 10.1111/j.1523-1755.1998.00824.x
13. Wong EK, Anderson HE, Herbert AP, et al. Characterization of a factor H mutation that perturbs the alternative pathway of complement in a family with membranoproliferative GN. *J Am Soc Nephrol* (2014) 25(11):2425–33. doi: 10.1681/ASN.2013070732
14. Ferreira VP, Herbert AP, Cortes C, et al. The binding of factor H to a complex of physiological polyanions and C3b on cells is impaired in atypical hemolytic uremic syndrome. *J Immunol* (2009) 182(11):7009–18. doi: 10.4049/jimmunol.0804031
15. Pechtl IC, Kavanagh D, McIntosh N, et al. Disease-associated N-terminal complement factor H mutations perturb cofactor and decay-accelerating activities. *J Biol Chem* (2011) 286(13):11082–90. doi: 10.1074/jbc.M110.211839
16. Yu Y, Triebwasser MP, Wong EK, et al. Whole-exome sequencing identifies rare, functional CFH variants in families with macular degeneration. *Hum Mol Genet* (2014) 23(19):5283–93. doi: 10.1093/hmg/ddu226
17. Raychaudhuri S, Iartchouk O, Chin K, Tan PL, Tai AK, Ripke S, et al. A rare penetrant mutation in CFH confers high risk of age-related macular degeneration. *Nat Genet* (2011) 43(12):1232–6. doi: 10.1038/ng.976
18. Whaley K, Ruddy S. Modulation of C3b hemolytic activity by a plasma protein distinct from C3b inactivator. *Science* (1976) 193(4257):1011–3. doi: 10.1126/science.948757
19. Schmidt CQ, Herbert AP, Kavanagh D, Gandy C, Fenton CJ, Blaum BS, et al. A new map of glycosaminoglycan and C3b binding sites on factor H. *J Immunol* (2008) 181(4):2610–9. doi: 10.4049/jimmunol.181.4.2610
20. Caprioli J, Noris M, Brioschi S, et al. Genetics of HUS: the impact of MCP, CFH, and IF mutations on clinical presentation, response to treatment, and outcome. *Blood* (2006) 108(4):1267–79. doi: 10.1182/blood-2005-10-007252
21. Kavanagh D, Richards A, Goodship T, et al. Transplantation in atypical hemolytic uremic syndrome. *Semin Thromb Hemost* (2010) 36(6):653–9. doi: 10.1055/s-0030-1262887
22. Merinero HM, Garcia SP, Garcia-Fernandez J, Arjona E, Tortajada A, Rodriguez de Cordoba S. Complete functional characterization of disease-associated genetic variants in the complement factor H gene. *Kidney Int* (2018) 93(2):470–81. doi: 10.1016/j.kint.2017.07.015
23. Kavanagh D, Goodship TH, Richards A. Atypical hemolytic uremic syndrome. *Semin Nephrol* (2013) 33(6):508–30. doi: 10.1016/j.semnephrol.2013.08.003
24. Lehtinen MJ, Rops AL, Isenman DE, van der Vlag J, Jokiranta TS. Mutations of factor H impair regulation of surface-bound C3b by three mechanisms in atypical hemolytic uremic syndrome. *J Biol Chem* (2009) 284(23):15650–8. doi: 10.1074/jbc.M900814200
25. Triebwasser MP, Roberson ED, Yu Y, et al. Rare Variants in the Functional Domains of Complement Factor H Are Associated With Age-Related Macular Degeneration. *Invest Ophthalmol Vis Sci* (2015) 56(11):6873–8. doi: 10.1167/iovs.15-17432
26. Hocking HG, Herbert AP, Kavanagh D, et al. Structure of the N-terminal region of complement factor H and conformational implications of disease-linked sequence variations. *J Biol Chem* (2008) 283(14):9475–87. doi: 10.1074/jbc.M709587200
27. Kerr H, Wong E, Makou E, et al. Disease-linked mutations in factor H reveal pivotal role of cofactor activity in self-surface-selective regulation of complement activation. *J Biol Chem* (2017) 292(32):13345–60. doi: 10.1074/jbc.M117.795088
28. Tortajada A, Montes T, Martinez-Barricarte R, et al. The disease-protective complement factor H allotypic variant Ile62 shows increased binding affinity for C3b and enhanced cofactor activity. *Hum Mol Genet* (2009) 18(18):3452–61. doi: 10.1093/hmg/ddp289
29. Licht C, Heinen S, Jozsi M, et al. Deletion of Lys224 in regulatory domain 4 of Factor H reveals a novel pathomechanism for dense deposit disease (MPGN II). *Kidney Int* (2006) 70(1):42–50. doi: 10.1038/sj.ki.5000269
30. Bruel A, Kavanagh D, Noris M, et al. Hemolytic Uremic Syndrome in Pregnancy and Postpartum. *Clin J Am Soc Nephrol* (2017) 12(8):1237–47. doi: 10.2215/CJN.00280117
31. Servais A, Noel LH, Roumenina LT, et al. Acquired and genetic complement abnormalities play a critical role in dense deposit disease and other C3 glomerulopathies. *Kidney Int* (2012) 82(4):454–64. doi: 10.1038/ki.2012.63
32. Fritsche LG, Igl W, Bailey JN, Grassmann F, Sengupta S, Bragg-Gresham JL, et al. A large genome-wide association study of age-related macular degeneration highlights contributions of rare and common variants. *Nat Genet* (2016) 48(2):134–43. doi: 10.1038/ng.3448
33. Wong EKS, Stout J, Ndebele J, Watt A, Malina M, Johnson S, et al. The Annual Report of the National Renal Complement Therapeutics Centre 2017/18. (2018).
34. Duvvari MR, Saksens NT, van de Ven JP, de Jong-Hesse Y, Schick T, Nillesen WM, et al. Analysis of rare variants in the CFH gene in patients with the cuticular drusen subtype of age-related macular degeneration. *Mol Vis* (2015) 21:285–92.
35. Fremeaux-Bacchi V, Fakhouri F, Garnier A, et al. Genetics and outcome of atypical hemolytic uremic syndrome: a nationwide French series comparing children and adults. *Clin J Am Soc Nephrol* (2013) 8(4):554–62. doi: 10.2215/CJN.04760512
36. Xue X, Wu J, Ricklin D, Forneris F, Di Crescenzio P, Schmidt CQ, et al. Regulator-dependent mechanisms of C3b processing by factor I allow differentiation of immune responses. *Nat Struct Mol Biol* (2017) 24(8):643–51. doi: 10.1038/nsmb.3427
37. Kavanagh D, Anderson HE. Interpretation of genetic variants of uncertain significance in atypical hemolytic uremic syndrome. *Kidney Int* (2012) 81(1):11–3. doi: 10.1038/ki.2011.330
38. Wu J, Wu YQ, Ricklin D, Janssen BJ, Lambris JD, Gros P. Structure of complement fragment C3b-factor H and implications for host protection by complement regulators. *Nat Immunol* (2009) 10(7):728–33. doi: 10.1038/ni.1755
39. Recalde S, Tortajada A, Subias M, et al. Molecular Basis of Factor H R1210C Association with Ocular and Renal Diseases. *J Am Soc Nephrol* (2016) 27(5):1305–11. doi: 10.1681/ASN.2015050580
40. Janssen van Doorn K, Dirinck E, Verpooten GA, Couttenye MM. Complement factor H mutation associated with membranoproliferative glomerulonephritis with transformation to atypical haemolytic uraemic syndrome. *Clin Kidney J* (2013) 6(2):216–19. doi: 10.1093/ckj/sfs190

Conflict of Interest: EKSW has received consultancy income from Alexion Pharmaceuticals, Biocryst, and Novartis. KJM, has received consultancy income from Gemini Therapeutics Freeline Therapeutics, MPM Capital, Catalyst Biosciences. CLH has received consultancy income from Roche, GSK, Gyroscope Therapeutics, Q32 Bio, Freeline Therapeutics, Ra Pharmaceuticals, and Biocryst. DK has received consultancy income from Gyroscope Therapeutics, Alexion Pharmaceuticals, Novartis, Apellis and Sarepta.

The remaining authors declare that the research was conducted in the absence of any commercial or financial relationships that could be construed as a potential conflict of interest.